

Dynamics of density fluctuations of a glass-forming epoxy resin revealed by Brillouin light scattering

D. Fioretto, L. Comez, G. Socino, and L. Verdini

INFN and Dipartimento di Fisica, Università di Perugia, I-06100 Perugia, Italy

S. Corezzi and P. A. Rolla

INFN and Dipartimento di Fisica, Università di Pisa, I-56126 Pisa, Italy

(Received 14 May 1998; revised manuscript received 15 July 1998)

Brillouin light scattering is used for studying the spectrum of density fluctuations of the glass-forming epoxy resin diglycidyl ether of bisphenol-A. Spectra at different temperatures ranging from the glassy to the liquid phase are obtained from a direct subtraction of depolarized from polarized spectra. In addition to the structural relaxation, evidence is given of a fast secondary relaxation process, which affects Brillouin spectra also at temperatures lower than that of the glass transition T_g . For the elaboration of isotropic spectra, we exploit the possibility of using the same relaxation function gained from dielectric spectra taken from the same sample. The temperature behavior of the relaxation strength shows the existence of an onset for the structural relaxation, located at a temperature about 93 K higher than T_g , consistent with the results of previous dielectric spectroscopy and depolarized light scattering investigations. The role of secondary relaxations of intramolecular nature in the mode-coupling analysis of real glass formers is also discussed. [S1063-651X(99)12601-1]

PACS number(s): 64.70.Pf, 78.35.+c, 83.50.Fc

I. INTRODUCTION

Density fluctuations play a central role in the dynamics of glass forming systems. The glass transition itself is associated to the blocking of long time density fluctuation, driving the system from the metastable supercooled phase to the nonergodic glassy state. [1]

Inelastic neutron, x ray, and light scattering are the most widely used techniques for studying the dynamics of density fluctuations in supercooled systems. Among these techniques, Brillouin light scattering (BLS) is a powerful tool for the determination of the spectrum of density fluctuations in the GHz frequency region and it has been extensively used to investigate glass-forming systems. Materials previously studied include fragile systems, such as propylene carbonate (PC) [2,3], CaKNO_3 [4], metacresylphosphate (*m*-TCP) [5], *o*-terphenyl (OTP) [6], LiCl solutions [7], salol [8,9], polybutadiene (PB) [10,11], polyacrylates [12], intermediate systems as GeSBr_2 [13], ZnCl_2 [14] and strong systems, as B_2O_3 [15]. In the early works, only the frequency shifts and linewidths of Brillouin peaks were analyzed, losing the information contained in the detailed shape of Brillouin peaks and in the central part (Mountain) of the spectrum. More recent studies have taken advantage of multipass tandem interferometers which, with respect to more traditional setups, are characterized by high contrast and resolution and by a considerably enlarged accessible frequency region. Thanks to this improvement, the full spectrum analysis can be profitably carried out by means of generalized hydrodynamics. In the same years, the mode coupling theory (MCT) [1] has been proposed as the first microscopic model of the glass transition, giving a renewed impulse to this research. Actually, MCT predicts nonlinear effects in the dynamics of density fluctuations of supercooled systems to become evident just in the spectral region covered by BLS, for temperatures

50–100 K higher than the traditionally defined glass transition temperature T_g . These nonlinearities are claimed to be responsible for the structural arrest, i.e., for a dynamic transition located at $T_c > T_g$, similar to that found in the study of spin glasses [16], where the transition from ergodic to nonergodic behavior occurs. A quantitative signature of this transition is expected in the Debye-Waller factor f_q , which shows a square root cusp in its temperature behavior at T_c [1]. In the $Q \rightarrow 0$ limit of light scattering, f_0 can be obtained as $f_0 = 1 - c_0^2/c_\infty^2$ [1] where c_0 and c_∞ are the relaxed and unrelaxed sound velocities, respectively.

In order to test the MCT predictions, a number of experiments have been performed by depolarized light scattering (DLS) [1,4,17–19], while a minor role has been ascribed to polarized light scattering. It could appear a paradox to use depolarized scattering, whose coupling with density fluctuations is still debated [20], to test the predictions of a theory which mainly concerns with the dynamics of density fluctuations. The main reason can be found in the very wide frequency window of about 12 decades which can be “easily” accessed by DLS, to be compared with the 1–2 decades detected by BLS. As a consequence of the narrow frequency range, the condition for getting information from BLS spectra is the *a priori* guess of the most appropriate memory function. It has been demonstrated that different choices for the memory function can lead to very different results for the values of the relevant relaxation parameters (see, for instance, the case of propylene carbonate of Refs. [2,3]). A very promising route for the interpretation of polarized spectra has been recently proposed by Cummins and co-workers in the case of CaKNO_3 [4], where an empirical memory function was constructed, obtained by a previous DLS study of the same system. The basic idea which underlies this procedure is the supposed “universal” shape of the memory functions of an undercooled system. Different theories, in-

cluding MCT, predict this universality, supported by a number of convincing experimental evidence [1]. In the present paper, we further develop this procedure by a careful analysis of the low frequency region of the spectrum (mountain) and by exploiting the relaxation function obtained by wide-band dielectric spectroscopy measurements.

The system here studied, the epoxy resin diglycidyl ether of bisphenol-A (DGEBA), is a fragile liquid that is particularly appropriate for this investigation. In fact, it does not exhibit any appreciable crystallization also at the slowest cooling rates, it gives a strong depolarized signal suitable for depolarized light scattering [21] and it has a dipole moment associated with the epoxy rings, which allows a detailed dielectric investigation over a wide frequency and temperature range [22,25]. Knowledge of the memory functions obtained by both DLS and DS, makes DGEBA a good candidate for a deeper BLS investigation.

In Sec. II the experiment is described, together with the procedure adopted to obtain the spectrum of density fluctuations from combined polarized and depolarized spectra. In Sec. III the spectrum of density fluctuations is analyzed giving a direct evidence of the sensitivity of BLS to secondary relaxations occurring in supercooled and glassy DGEBA. A particular attention is paid to the analysis of the mountain region of the spectrum that is usually neglected and that is shown to give important information on the most appropriate memory function. The shape of the mountain region is demonstrated to be consistent with that obtained by DS measurements performed on the same system. Through use of the relaxation function obtained from dielectric spectra, the full fitting of BLS spectra has been successfully performed. The results of the fitting support the idea of a change in the dynamics of the glass forming system as recently observed in different supercooled liquids [23,24]. In the same section we also discuss some possible consequences of the reported findings, with particular attention to the possibility of a MCT analysis of BLS data of “real” glass formers, such as DGEBA, OTP, PC, and PB. Our conclusions are given in Sec. IV.

II. EXPERIMENT

The epoxy resin here examined is a commercial sample of diglycidyl ether of bisphenol-A (DGEBA) with an epoxy equivalent weight of about 190. The sample was filtered through a 0.22 μm membrane. Polarized I_{\parallel} and depolarized I_{\perp} spectra were recorded in the backscattering ($\theta=180^\circ$) geometry for temperatures between 223 and 343 K, i.e., above and close to the glass transition temperature $T_g=257$ K. The temperature fluctuations were kept within ± 0.1 K during the spectra recording. An Ar^+ laser was used operating at a power of ≈ 200 mW on a single mode of the 514.5-nm line. The light scattered by the sample was analyzed by means of a Sandercock type (3+3)-pass tandem Fabry-Perot interferometer characterized by a finesse approximately 100 and a contrast ratio greater than 5×10^{10} [26]. A dilute aqueous suspension of standard latex particles was used to determine the instrumental function.

Both \parallel and \perp spectra are required to obtain the spectrum of density fluctuations $I_{\rho\rho}$, which is proportional to the dynamic structure factor $S(q, \omega)$. In fact, the Brillouin spec-

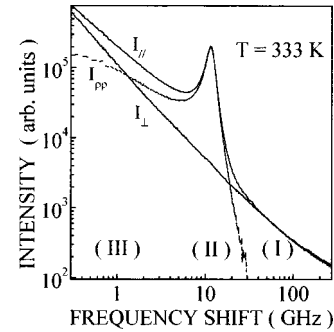


FIG. 1. Log-log plot of I_{\parallel} , I_{\perp} , and $I_{\rho\rho}$ spectra at $T=333$ K. The $I_{\rho\rho}$ spectrum is obtained by subtracting the appropriate anisotropic scattering contribution from the I_{\parallel} spectrum, as discussed in the text.

trum I_{\parallel} is the sum between the isotropic spectrum $I_{\rho\rho}(\omega)$ and a contribution from anisotropic scattering, while the \perp spectrum I_{\perp} consists of the latter contribution only. Neglecting thermal fluctuations, the isotropic spectrum is the sum of the density fluctuation spectrum $I_{\rho\rho}$ and isotropic induced contributions [27]. In the case of negligible contribution from induced isotropic terms, measurements of both I_{\parallel} and I_{\perp} spectra yields the density fluctuation spectrum, according to the equation [28]:

$$I_{\rho\rho}(\omega) = I_{\parallel}(\omega) - r^{-1}I_{\perp}(\omega). \quad (2.1)$$

where r is the depolarization ratio and $\omega = 2\pi\nu$ where ν is the frequency shift of Brillouin spectra. It has to be noticed that at temperatures close and below T_g also transverse acoustic waves contribute to the depolarized spectrum, as reported in a previous work [29]. However, in the backscattering configuration here adopted, this latter q -dependent contribution vanishes and Eq. (2.1) can be used both in the liquid and the glassy phase.

As for the parameter r entering Eq. (1), it has to be measured at each temperature. This is a nontrivial task when using active stabilization interferometers, i.e., in the case of multipass tandem interferometers. In order to overcome this difficulty, we observe that the $S(q, \omega)$ contribution to the \parallel spectrum generally goes to zero for frequencies higher than 30 or 40 GHz, so that above these values the \parallel and \perp spectra have the same shape. By taking spectra up to frequencies higher than 40 GHz and multiplying I_{\perp} by an appropriate factor, it is thus possible to overlap the high frequency tails of I_{\perp} and I_{\parallel} . This procedure is illustrated in Fig. 1 for the case $T=333$ K. The two spectra can then be directly subtracted to obtain $I_{\rho\rho}$, as shown in the figure, thus avoiding an explicit evaluation of r . The figure also shows that the anisotropic scattering appreciably contributes to the shape of the \parallel spectra, especially at frequencies lower than the Brillouin peak position, thus emphasizing the necessity of the subtraction procedure.

In order to obtain high resolution spectra sufficiently extended in frequency, we typically joined, for each polarization and temperature, four spectra collected with the different free spectral ranges (FSR) of 7.5, 10, 37.5, and 300 GHz. In the case of FSR=7.5 GHz, spectra have been taken using different pinhole widths of 100, 200, and 400 microns. By a comparison of the low frequency parts of the spectra it was

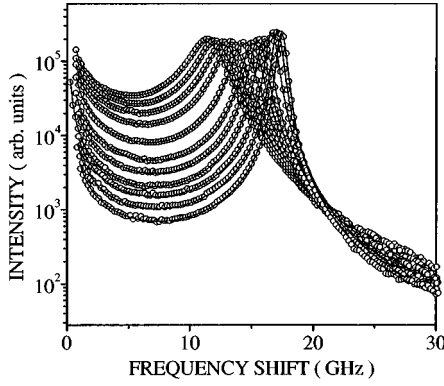


FIG. 2. $I_{\rho\rho}$ spectra. The solid lines represent the fits to the data obtained as explained in the text, using Eq. (3.2).

possible to identify the contribution of the elastic line and to determine the low frequency limit of the scattered spectrum which, in the present case, is between 0.2 and 0.3 GHz.

The temperature behavior of the relaxed sound velocity c_0 has been measured by means of an ultrasonic technique [30], which operates in the range 1–3 MHz, i.e., at frequencies which are four orders of magnitude lower than those of acoustic modes revealed by BLS. A PZT transducer was placed deep into the sample, at a distance $L=5$ mm from the bottom of a brass cell parallel to the surface of the transducer. The system as a whole works as an acoustic Fabry-Perot, so that the reflection coefficient $R(f)$ shows a series of minima corresponding to the condition $L=m\Lambda/2$, where Λ is the acoustic wavelength and m is an integer number. The reflection coefficient was measured as a function of frequency by means of a network analyzer. The frequency distance Δf between two neighboring minima, i.e., the free spectral range of the acoustic Fabry-Perot interferometer, is given by the relation $\Delta f=c/2L$ and the Fourier transform of $R(f)$ shows a well defined maximum at $t=2L/c$, where c is the velocity of the acoustic wave in the sample. From measurement of t the velocity c of longitudinal acoustic waves could be thus obtained at different temperatures in the range 303–353 K.

III. RESULTS AND DISCUSSION

The dynamic structure factor obtained by the procedure outlined in the previous section is shown in Fig. 2 for different temperatures. In all the reported cases we found a linewidth of the Brillouin peaks larger than the instrumental function and a non-negligible quasielastic (mountain) contribution. These results suggest the presence, in this frequency region, of some relaxation process different from the structural relaxation which, for temperatures close to T_g , is located at a frequency approximately ten orders of magnitude lower.

The relationship for the dynamic structure factor can be derived from the equation of motion of the density fluctuations $\rho_q(t)$. Neglecting the thermal diffusion mode and its contribution to the acoustic mode damping, the linearized hydrodynamic equations [31,32] give:

$$\ddot{\rho}_q(t) + \left(\frac{\eta_L}{\rho} q^2\right) \dot{\rho}_q(t) + \left(\frac{M}{\rho} q^2\right) \rho_q(t) = 0, \quad (3.1)$$

where ρ is the static mass density η_L is the longitudinal viscosity, M is the adiabatic compressional modulus and q is linked to the wave number of the incident light k_i and to the refractive index of the medium n by the relationship $q=2nk_i$. In supercooled liquids, relaxation processes such as structural and secondary relaxations, influence the dynamics of the system. The presence of these relaxations can be taken into account through a frequency dependent longitudinal modulus $M(\omega)=M'(\omega)-iM''(\omega)$. The spectrum of density fluctuations can be thus calculated from Eq. (3.1), through the fluctuation-dissipation theorem:

$$I_{\rho\rho}(\omega) = \frac{I_0}{\omega} \frac{M''(\omega) + \omega \eta_L}{[\omega^2 \rho/q^2 - M'(\omega)]^2 + [M''(\omega) + \omega \eta_L]^2} \quad (3.2)$$

where the term $\omega \eta_L$ is frequently included into $M''(\omega)$. This spectrum shows a maximum close to the characteristic frequency of longitudinal acoustic (LA) modes $\omega_{LA}=(M'q^2/\rho)^{1/2}$, corresponding to the peaks at approximately 10 GHz of Fig. 2. From a careful inspection of Eq. (3.2) and of Fig. 1, three main regions can be recognized in the spectrum: (I) a high frequency region $\omega \gg \omega_{LA}$ where the spectrum shows a steep decrease; (II) an intermediate region $\omega \approx \omega_{LA}$ around the peak of LA modes; (III) a low frequency region around the peak centered at zero frequency, usually referred to as the mountain mode. A more detailed analysis of these regions is reported in the following, since each of them gives some peculiar information on the dynamics of the system and suggests a possible route for the whole spectrum analysis of Brillouin spectra.

A. High frequency, $\omega \gg \omega_{LA}$

In this frequency region, the spectrum quickly goes to zero. In the case of a simple Debye relaxation, i.e., $M(\omega)=M_\infty-\Delta/(1+i\omega\tau)$ where M_∞ and Δ are the unrelaxed modulus and the relaxation strength, respectively, Eq. (3.2) shows a ω^{-6} behavior for $\omega \gg \omega_{LA}$, τ^{-1} . In the more general case, the value of the exponent can be different but the trend to zero of the spectrum for $\omega > \omega_{LA}$ remains a general feature. In this region, the dominant contribution to the polarized spectrum is thus given by the anisotropy fluctuations, thus justifying the subtraction procedure previously outlined.

B. Medium frequency, $\omega \approx \omega_{LA}$

The region (II) in the spectrum of Fig. 1 is located around the peak of the LA mode. This is the part of the Brillouin spectrum that is traditionally analyzed since, when using nontandem interferometers, the frequency position and the width of LA peaks undergo a negligible distortion by the overlapping of different orders of the interferometer. Position and width of the peaks give velocity and attenuation of the longitudinal modes, i.e., real (M') and imaginary (M'') parts of the longitudinal modulus. In fact, for frequencies close to the peak, the spectrum of Eq. (3.2) can be approximated by that of a damped harmonic oscillator (DHO):

$$I_{LA}(\omega) = I_{LA}^0 \frac{\Gamma_{LA} \omega_{LA}^2}{[\omega_{LA}^2 - \omega^2]^2 + [\omega \Gamma_{LA}]^2}, \quad (3.3)$$

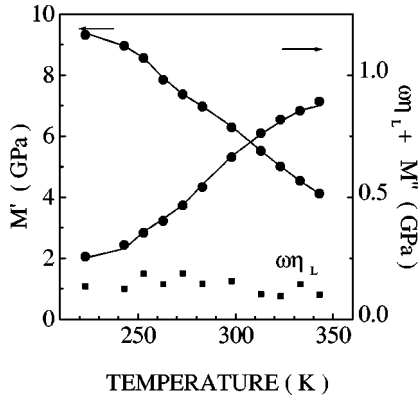


FIG. 3. Real and imaginary parts of the longitudinal acoustic modulus obtained from frequency position and linewidth of Brillouin peaks, using Eq. (3.4). Squares represent the separate contribution of longitudinal viscosity to the linewidth.

where ω_{LA}^2 and Γ_{LA} approximately correspond to the frequency position and to the full width at half maximum (FWHM) of LA peaks. These parameters are related to the real and imaginary parts of the longitudinal modulus through the relations

$$M'(\omega_{LA}) = \rho \omega_{LA}^2 / q^2, \quad (3.4a)$$

$$M''(\omega_{LA}) + \omega_{LA} \eta_L = \rho \omega_{LA} \Gamma_{LA} / q^2. \quad (3.4b)$$

We performed the fits of Eq. (3.3) convoluted with the instrumental function to the experimental spectra in a narrow region around the LA peaks by means of the standard Levenberg-Marquardt routine. The values of ω_{LA} and Γ_{LA} obtained by this procedure were used in Eq. (3.4) to calculate the values of the longitudinal modulus and the results are reported in Fig. 3.

Inspection of the figure shows that the temperature behavior of $M(\omega_{LA})$ changes near the glass transition temperature of the resin $T_g = 257$ K previously determined by calorimetric and dielectric measurements [22]. BLS can in fact be used as a local probe of the glass transition, as recently shown for thin polymeric films [33]. Moreover, it can be seen that $M''(\omega_{LA})$, which is proportional to the mechanical losses in the system, increases with increasing temperature. The origin of the mechanical losses in supercooled systems can be attributed to the presence of a structural relaxation, frequently accompanied by one or more secondary relaxation processes. The structural relaxation is related to a cooperative diffusion motion of molecules. Its characteristic time diverges when approaching the glass transition, so that the absorption and dispersion regions progressively move toward lower frequencies, leaving the BLS frequency region. Different from this, a secondary relaxation is associated to a more localized and faster motion of the molecules, which remains activated also at temperatures lower than T_g . In the present case, since $M''(\omega_{LA})$ is considerably greater than zero even at temperatures lower than T_g , the absorption can be attributed to a secondary relaxation processes. This gives evidence of the sensitivity of BS to the secondary relaxation of DGEBA, which will be confirmed in the following by both the low frequency and the full spectrum analysis.

So far, BLS has been used as an ultrasonic technique to obtain the viscoelastic characterization of the supercooled liquid, i.e., to measure the temperature behavior of the real and imaginary part of the longitudinal modulus of the liquid, at the single frequency of the Brillouin peak in the spectra. The main difference with respect to more traditional ultrasonic methods is the frequency region around 10 GHz, difficult to access by other techniques. The main limit of this analysis is that it cannot discriminate the nature and the number of relaxation processes which contribute to the acoustic loss and dispersion. To gain this information, the frequency dependence of the modulus is required. In the case of Brillouin spectroscopy, the estimation of the frequency dependence of the elastic modulus at each temperature can be obtained in a frequency region of about two decades by means of a full spectrum analysis. The fit of the whole spectrum by Eq. (3.2) require the functional shape of the relaxation function of $M(\omega)$ to be known. In order to get this information, a careful analysis of the low frequency region of the spectrum can be fruitful.

C. Low frequency, $\omega \ll \omega_{LA}$

The low frequency region of Brillouin spectra gives a direct access to the shape of the relaxation function. In fact, for $\omega \ll \omega_{LA}$ and for a contribution from viscosity $\omega \eta_L$ negligible with respect to that of $M''(\omega)$, the spectrum of Eq. (3.2) can be approximated by

$$I_{\rho\rho}(\omega) = \frac{I_0}{\omega} \frac{M''(\omega)}{M'(\omega)^2 + M''(\omega)^2} = \frac{I_0}{\omega} \text{Im}\{J(\omega)\}, \quad (3.5)$$

where $J(\omega)$ is the inverse of the longitudinal modulus, i.e., a longitudinal compliance. This equation shows that the imaginary part of the longitudinal compliance can be directly obtained from the low frequency part of the spectrum of density fluctuations. This part of the spectrum gives an important piece of information on the dynamics of the sample, i.e., the frequency dependence of the relaxation function of density fluctuations, which can be directly compared with both the prediction of theories of supercooled liquids and with the results obtained by different spectroscopic investigations. The high frequency limit of this spectral region is determined by the position of the LA peak. The backscattering configuration here adopted gives the highest value of the exchanged momentum q , corresponding to the highest frequency position of the LA peak at the chosen wavelength of the laser light. The low frequency limit of the analyzed spectral region is mainly given by the resolution of the FP interferometer which, in the present case, is of some hundred MHz. The width of this spectral region is thus approximately one decade, enough to give information on the shape of the relaxation function. In Fig. 4 we report the compliance deduced from $I_{\rho\rho}$ spectra as a function of frequency for different values of temperature. These spectra are normalized to the imaginary part of the dielectric function (which is also a compliance) measured in the same system. The agreement between the frequency behavior of the two quantities is noticeable in the whole temperature range and lead us to infer that the shape of the relaxation functions is the same, within the experimental errors, for both dielectric

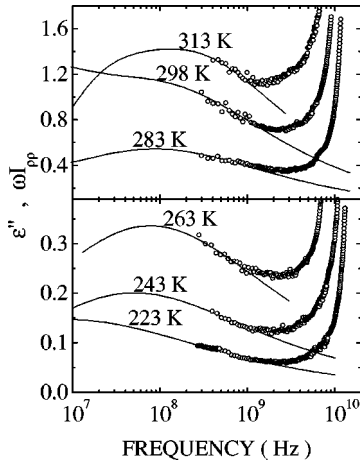


FIG. 4. Comparison between dielectric spectra (full lines) and longitudinal compliance (open circles) obtained from the low frequency part of I_{pp} spectra by means of Eq. (3.5).

and Brillouin measurements of compliance. This result brings a couple of relevant consequences.

(i) From the direct comparison between Brillouin and dielectric data we have the evidence that BS is effective in revealing the dynamics of secondary relaxations. In fact, dielectric measurements show the presence of two relaxations in this system: the structural relaxation that is visible in the low frequency part of the spectra for temperatures higher than 298 K and rapidly moving toward lower frequencies for decreasing temperature, and a strong secondary relaxation, usually associated with the rotation of the epoxy rings of the molecules, located in the 100 MHz region, with a relaxation time that is slowly temperature dependent. This secondary relaxation is present in the spectra of both the supercooled and the glassy phases and is the only one to be present in the frequency region of Fig. 4 for temperatures lower than 283 K. The presence of a relaxation in BS spectra gives clear evidence of the sensitivity of BS to secondary processes and is consistent with the previously reported finite value of $M''(\omega_{LA})$ near the glass transition.

(ii) The obtained results suggest an interesting route for a further elaboration of Brillouin spectra, consisting of the use of the same relaxation functions deduced from DS for the full spectrum analysis of BS spectra. This allows to take properly into account the contributions of both structural and secondary relaxations and to achieve a better insight into the dynamics of the system. We notice that, in the present case, the use of a relaxation function deduced from depolarized light scattering [4] would not be suitable for fitting Brillouin spectra since it has been shown [21] that such a function does not show any evidence of the secondary relaxation revealed by both BLS and DS. As a possible reason for the absence of secondary relaxation in DLS spectra, we notice that the part of the molecule that is mainly responsible for DLS is the inner one, where two phenyl rings are located. This part does not directly participate in the motion of the external epoxy groups, i.e., the secondary relaxation.

D. Full spectrum analysis

According to the procedure used for dielectric spectra of DGEBA, the longitudinal compliance measured by Brillouin spectra has been written as the sum of two HN functions [34]:

$$J(\omega) = J_2 + \frac{J_0 - J_1}{[1 + (i\omega\tau_1)^{\alpha_1}]^{\gamma_1}} + \frac{J_1 - J_2}{[1 + (i\omega\tau_2)^{\alpha_2}]^{\gamma_2}} \quad (3.6)$$

where J_0 , J_1 and J_2 are related to the relaxed (c_0), intermediate (c_1), and unrelaxed (c_2) sound velocities, respectively, through the relation $J = 1/\rho c^2$, τ_1 and τ_2 are the relaxation times, α_1, γ_1 and α_2, γ_2 the shape parameters of the primary and secondary relaxation, respectively. The reasons of the success of the HN phenomenological law in fitting the relaxation data of many glass forming systems [35,36] can be summarized as follows. This function interpolates two power law regimes: A low frequency power law $J''(\omega) \propto \omega^m$ characterized by the exponent $m = \alpha$ in Eq. (3.6), and the high frequency $J''(\omega) \propto \omega^{-n}$ with $n = \alpha\gamma$. The existence of these power law regimes is a well known feature of complex systems [37] and has been also recently predicted by theories of supercooled liquids, such as the mode coupling theory [1]. Moreover, the HN function gives a good Fourier transform of the time domain KWW relaxation function [38], which has been found to describe the time evolution of correlation and relaxation functions of glass forming liquids.

Inspection of Eq. (3.6) shows that the whole set of relaxation parameters is rather large and it would be difficult to determine their values by a single experimental spectrum. The observed coincidence of the shape of BS and DS compliances suggests the use of the values of the shape parameters α_1 , γ_1 , α_2 , and γ_2 previously obtained by DS measurements for fitting BS spectra. Also the value of τ_1 has been taken equal to that obtained by DS, since in the whole temperature range here analyzed, it is located at a frequency too low to be determined by the fitting. In order to further reduce the number of free parameters, the temperature behavior of c_0 has been measured by the previously described ultrasonic technique [30] in the range 303–353 K. These data show a linear behavior for $T > 310$ K and a dispersion similar to that observed by BLS at lower temperatures. The linear region gives the temperature behavior of the relaxed sound velocity $c_0(T) = [2.75 - 0.00375T(\text{K})] \text{ km s}^{-1}$. The relaxation parameters that are to be determined by the fitting of the whole Brillouin spectrum are therefore η_L , τ_2 , c_1 , and c_2 .

The spectra at different temperatures have been fitted by Eq. (3.2) where the modulus $M(\omega)$ was written in terms of the compliance $J(\omega)$ of Eq. (3.6), as $M(\omega) = 1/J(\omega)$. The results of the fitting procedure are reported as solid lines in Fig. 2. The goodness of the fit in the whole frequency and temperature range is a proof of the consistency of the elaboration procedure. A further proof is provided by the data of the real and imaginary parts of the longitudinal modulus previously obtained from the frequency position and linewidth of Brillouin peaks, which are reported in Fig. 3 together with those obtained by the full spectrum analysis. The values of $M'(\omega_{LA})$ and $M''(\omega_{LA})$ have been calculated at each temperature from Eq. (3.6) using the relaxation parameters obtained by the fit and the results are reported in Fig. 3 as a full line. In this same figure the contribution of viscosity $\omega\eta_L$ to M'' is also separately shown. The values of $\omega\eta_L$ obtained by the fit are in the range $\omega\eta_L = 0.13 \pm 0.03$ GPa in the whole investigated temperature region. It can be seen that also at

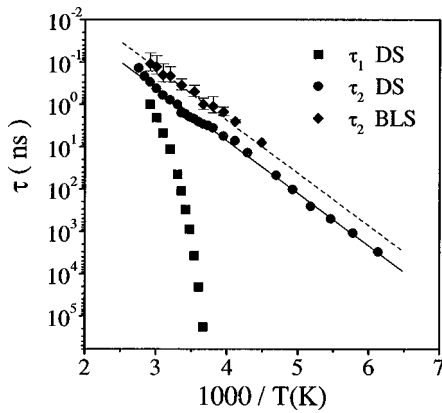


FIG. 5. Temperature dependence of relaxation times of DGEBA. Squares represent the structural relaxation revealed by dielectric spectroscopy, circles and diamonds the secondary relaxation obtained by dielectric and $I_{\rho\rho}$ spectra, respectively.

the lowest investigated temperatures this viscosity cannot completely account for the elastic loss, which is consistent with the presence of a high frequency relaxation process in the system.

The values obtained for τ_2 are reported in Fig. 5, together with those of τ_1 and τ_2 of previous dielectric measurements. The dielectric values of τ_2 were fitted by the Arrhenius law, $\tau_2(T) = \tau_{02} \exp(E_a/RT)$ (solid line in Fig. 5), where E_a is the activation energy per mole, R is the gas constant, and τ_{02} is the relaxation time in the high temperature limit. The following values of the parameters were obtained: $\tau_{02} = (7.0 \pm 2.7) \times 10^{-14}$ s and $E_a = (5.7 \pm 0.2)$ Kcal/mol. The values of the relaxation time obtained by BS can be interpolated by the dashed straight line in the figure, parallel to that of dielectric data, corresponding to an Arrhenius law with the same activation energy and with a limiting value of τ_{02} reduced by a factor of 3. The coincidence of the values of the activation energy confirms that dielectric spectroscopy and BS reveal the same relaxation process, which was related to the motion of the epoxy rings [39]. The difference between the value of τ_{02} relative to BLS and that obtained from dielectric spectra can be attributed to the different quantities measured by the two techniques. This difference is not in contradiction with the results of Fig. 4 and with the hypothesis of Eq. (3.6), i.e., the use of the same relaxation function deduced from DS for the full spectrum analysis of BS spectra. In fact, as previously discussed, the high frequency part of the HN relaxation function is the power law $J''(\omega) \propto \omega^{-n}$, which is self-similar for a change of the scale ω [40]. In other words, the coincidence of the high frequency parts of susceptibilities of Fig. 4 implies only a coincidence of the shape of the relaxation functions, not of the value of the time and of the relaxation strength (which, in fact, are free parameters in the fit).

It has to be noted that the Arrhenius behavior is a rather common result for the relaxation time obtained by BLS as found, for instance, in polyacrylates [12], polybutadiene [10,11] and polyurethane gels [41]. From these experimental findings one can deduce that BLS is particularly effective in revealing secondary relaxations in supercooled systems.

The values of c_1 and c_2 are reported in Fig. 6, together with those of c_0 obtained by the ultrasonic technique and

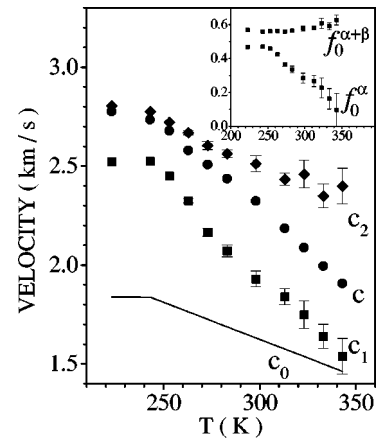


FIG. 6. Velocity of longitudinal acoustic waves in DGEBA. c_0 is the relaxed sound velocity obtained by ultrasonic measurements in the range 300–350 K; a linear extrapolation is assumed down to T_g and a constant value at lower temperatures. c_1 and c_2 are the intermediate and unrelaxed sound velocities, respectively, obtained from $I_{\rho\rho}$ spectra fitted by Eq. (3.2) and (3.6). c is the sound velocity at the frequency of the Brillouin peak, obtained from the values of M' of Fig. 4 by the equation $c = (M'/\rho)^{1/2}$. In the inset, the Debye-Waller factor is reported as defined in the text.

those of c deduced by the frequency position of the Brillouin lines. The values of c_1 progressively approach those of c_0 for increasing temperatures, i.e., the strength of the structural relaxation progressively decreases. This result is in qualitative agreement with the prediction of the MCT of a square root increase of the Debye-Waller factor f_0 for decreasing temperatures below the critical temperature T_c [1]. To better investigate this point, the temperature behavior of two possible definitions of this factor are reported in the inset of Fig. 6. In particular, we define $f_0^\alpha = 1 - c_0^2/c_1^2$ and $f_0^{\alpha+\beta} = 1 - c_0^2/c_2^2$. It can be seen that f_0^α accounts only for the strength of the structural relaxation, while $f_0^{\alpha+\beta}$ accounts for both structural and secondary relaxation. The decrease of f_0^α up to temperatures of approximately 300 K is consistent with the square root behavior predicted by the MC theory. For higher temperatures MCT predicts a cusp discontinuity, with f_0^α becoming constant with temperature. In the present case the slope of $f_0^\alpha(T)$ reduces at approximately 300 K, though it never attains the value zero predicted by the simplified version of the theory. On the other hand, the value of $f_0^{\alpha+\beta}$ is almost constant (or slightly increases) in the whole temperature range. The main message that comes out from this analysis, relevant to MCT, is that in “real” (nonideal) glass formers the intramolecular relaxations play an important role that cannot be ignored in the test of the theory. As a first approximation, we can deduce that f_0^α is the observable which better approximates the Debye-Waller factor described by the theory. It is important to recognize that these intramolecular relaxations are the rule, rather than an exception, in supercooled liquids. Also in the case of “prototypical” glass formers, such as OTP, clear signatures of such relaxations have been recently reported [6]. Of interest is also the case of polybutadiene, which has given the early experimental proofs of MCT [1] and, till now, has not shown any signature of the square root singularity in BLS investigations. Both our group [10] and, more recently, an indepen-

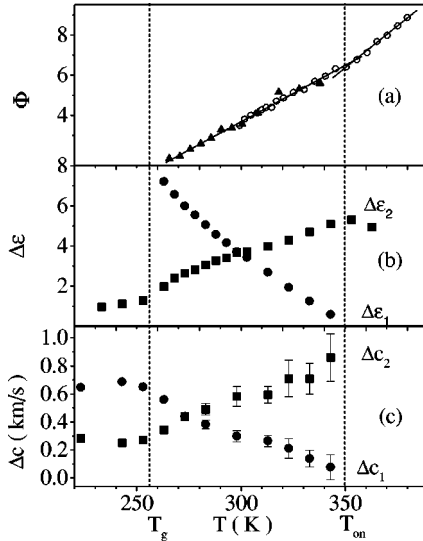


FIG. 7. Φ is the temperature derivative of the relaxation time $\Phi = [d(\log_{10}\tau^{-1})/dT]^{-1/2}$ obtained by both dielectric spectroscopy (triangles) and ion conductivity (open circles) measurements. $\Delta\epsilon_1$ ($\Delta c_1 = c_1 - c_0$) and $\Delta\epsilon_2$ ($\Delta c_2 = c_2 - c_1$) are the dielectric (acoustic) relaxation strengths of structural and secondary relaxation, respectively.

dent investigation [11] have reported a temperature independent value of f , similar to $f_0^{\alpha+\beta}$ of Fig. 6. Also in the case of PB, a well defined secondary relaxation has been evidenced by dielectric spectroscopy, which can be responsible for this behavior. Another interesting system is PC, for which the MCT analysis of the polarized spectrum was unsuccessful [3]. Also for PC there are evidences of a thermally activated secondary relaxation [42] which was not included in the BLS memory function. The results here reported for DGEBA suggest to reanalyze both PB and PC Brillouin spectra taking explicitly into account the presence of the secondary relaxation, which could recover the square root behavior of the MCT. In any case, a new version of MCT is demanded which also incorporates the intramolecular degrees of freedom, which are presently included neither in the idealized nor in the extended version of the theory.

The last step of our analysis concerns the onset of the structural relaxation process which can be inferred in the region 350–360 K, from the extrapolation of c_0 and c_1 data. This evidence is also supported by the temperature behavior of the dielectric relaxation strength of the structural relaxation [22], which goes to zero at $T_{on} \approx 350$ K. The consistency of dielectric results with those of light scattering suggests that this onset is an intrinsic feature of the dynamics of the system rather than an effect induced by the particular probe. At this same temperature, the splitting of structural and secondary relaxation times was observed (Fig. 5) together with a change of the temperature behavior of the main relaxation [25]. Some of these features are summarized in Fig. 7. The onset of the structural relaxation is evidenced by the progressive increase with decreasing temperature of both the dielectric and the acoustic relaxation strength [Figs. 7(b) and 7(c)]. The existence of a similar onset for the structural relaxation has been recently reported in poly(*n*-alkylmethacrylate)s [43], in polybutadiene [44], and in a simulation with a modified Fredrickson model [45]. The

change of the diffusive regime at T_{on} is also confirmed by the temperature derivative of the relaxation time obtained by both dielectric spectroscopy and ion conductivity reported in Fig. 7(a). Here $\Phi = [d(\log_{10}\tau^{-1})/dT]^{-1/2}$ shows a linear behavior when the relaxation time accomplishes to a Vogel-Fulcher (VF) law $\tau = \tau_0 \exp[DT_0/(T - T_0)]$. The marked change at $T = T_{on}$ means that the T behavior of τ_1 changes from a VF for $T > T_{on}$ to another one characterized by different values of the parameters for $T < T_{on}$ [23]. Depolarized light scattering measurements recently performed in DGEBA [21] show a transition near T_{on} from the Debye-Stokes (DS) diffusion law for $T > T_{on}$ to a fractional DS diffusion for $T < T_{on}$. The breakdown of the DS law in depolarized light scattering could be interpreted in terms of the fluctuation theory of the glass transition [46], i.e., of an onset of cooperative motions close to T_{on} with a cooperative volume that increases with decreasing temperature, diverging when approaching the Vogel temperature of the system.

These results, collected by different spectroscopic techniques, indicate that the change in the dynamics at T_{on} is, in a sense, a precursor of the glass transition since it is located at a temperature above T_g and marks the onset of the structural relaxation which, through the divergence of its characteristic time, defines the conventional temperature of the glass transition. Finally, we notice that the phenomenology here reported for DGEBA is also confirmed by dielectric and light scattering measurements presently in course in our laboratories on different epoxy systems.

IV. CONCLUSIONS

Spectra of density fluctuations of DGEBA have been obtained by Brillouin light scattering technique at different temperatures ranging from the glassy to the liquid phase. From the low frequency part of the spectrum, usually referred to as the Mountain region, direct evidence is given of a fast secondary relaxation process, which affects Brillouin spectra also at temperatures lower than that of the glass transition T_g . For the full spectrum analysis of Brillouin spectra, we have exploited the possibility of using the relaxation function previously obtained by dielectric spectroscopy measurements, consisting of the sum of structural and secondary relaxation. The activation energy of the secondary relaxation and the temperature behavior of the relaxation strength obtained by this elaboration procedure are consistent with those obtained by dielectric spectroscopy. In particular, from the decrease with temperature of the strength of the structural relaxation, the existence of an onset for this process has been inferred, located at a temperature about 93 K higher than T_g , consistent with dielectric spectroscopy and depolarized light scattering investigations performed on the same system.

Concerning the predictions of the mode coupling theory, and in particular the existence of a cusp in the temperature behavior of the nonergodicity factor f_0 , the analysis here reported opens a route for the interpretation of BLS data, which can lead to a reconciliation between theory and recent experimental findings in both epoxy systems and more studied glass forming systems, such as polybutadiene, orthoterphenyl, and propylene carbonate, which show intramolecular relaxations in the supercooled phase. As a first approximation, the presence of intramolecular relaxations can be ac-

counted by the use of phenomenological functions, such as that of Eq. (3.6) together with some ansatz on the shape of the function deduced from the low frequency part of the spectrum (mountain) and the comparison with susceptibilities obtained by different spectroscopic techniques. In order to give a full microscopic picture, a new version of MCT is strongly demanded which also incorporates the intramolecular degrees of freedom which are clearly demon-

strated to be effectively coupled to density fluctuations in real systems.

ACKNOWLEDGMENTS

It is a pleasure to thank Professor E. W. Fischer, Professor A. Patkowski, Professor G. Ruocco, Dr. G. Monaco, and Dr. W. Steffen for helpful discussions and suggestions.

-
- [1] W. Götze and L. Sjögren, *Rep. Prog. Phys.* **55**, 241 (1992).
- [2] M. Elmroth, L. Börjesson, and L. M. Torell, *Phys. Rev. Lett.* **68**, 79 (1992).
- [3] W. M. Du, G. Li, H. Z. Cummins, M. Fuchs, J. Toulouse, and L. A. Knauss, *Phys. Rev. E* **49**, 2192 (1994).
- [4] G. Li, W. M. Du, J. Hernandez, and H. Z. Cummins, *Phys. Rev. E* **48**, 1192 (1993).
- [5] M. Soltwisch, G. Ruocco, B. Balschun, J. Bosse, V. Mazzacurati, and D. Quitmann, *Phys. Rev. E* **57**, 720 (1998).
- [6] G. Monaco, L. Comez, and D. Fioretto, *Philos. Mag.* **B 77**, 463 (1998).
- [7] N. J. Tao, G. Li, and H. Z. Cummins, *Phys. Rev. B* **43**, 5815 (1991).
- [8] C. H. Wang and J. Zhang, *J. Chem. Phys.* **85**, 794 (1986).
- [9] C. Dreyfus, M. J. Lebon, H. Z. Cummins, J. Toulouse, B. Bonello, and R. M. Pick, *Phys. Rev. Lett.* **69**, 3666 (1992).
- [10] D. Fioretto, L. Palmieri, G. Socino, and L. Verdini, *Phys. Rev. B* **50**, 605 (1994).
- [11] A. Aoudi, M. J. Lebon, C. Dreyfus, B. Strube, W. Steffen, A. Patkowski, and R. M. Pick, *J. Phys.: Condens. Matter* **9**, 3803 (1997).
- [12] D. Fioretto, G. Carlotti, L. Palmieri, G. Socino, L. Verdini, and A. Livi, *Phys. Rev. B* **47**, 15 286 (1993); D. Fioretto, L. Palmieri, G. Socino, and L. Verdini, *J. Non-Cryst. Solids* **172-174**, 1130 (1994).
- [13] S. Loheider, G. Vögler, I. Petscherizin, M. Soltwisch, and D. Quitmann, *J. Chem. Phys.* **93**, 5436 (1990).
- [14] M. Soltwisch, J. Sukamanoutski, and D. Quitmann, *J. Chem. Phys.* **86**, 3207 (1987).
- [15] M. Grimsditch, R. Bhadra, and L. M. Torell, *Phys. Rev. Lett.* **62**, 2616 (1989).
- [16] T. R. Kirkpatrick and D. Thirumalai, *Phys. Rev. B* **36**, 5388 (1987); L. Cugliandolo and J. Kurchan, *Phys. Rev. Lett.* **71**, 173 (1993); S. Franz and G. Parisi, *ibid.* **79**, 2486 (1997).
- [17] H. Z. Cummins, G. Li, W. Du, R. M. Pick, and C. Dreyfus, *Phys. Rev. E* **53**, 896 (1996).
- [18] H. Z. Cummins, G. Li, W. Du, R. M. Pick, and C. Dreyfus, *Phys. Rev. E* **55**, 1232 (1997); M. J. Lebon, C. Dreyfus, G. Li, A. Aouadi, H. Z. Cummins, and R. M. Pick, *ibid.* **51**, 4537 (1995); H. Z. Cummins, G. Li, W. M. Du, J. Hernandez, and N. J. Tao, *J. Phys.: Condens. Matter* **6**, A51 (1994).
- [19] W. Steffen, A. Patkowski, H. Gläser, G. Meier, and E. W. Fischer, *Phys. Rev. E* **49**, 2992 (1994); W. Steffen, A. Patkowski, G. Meier, and E. W. Fischer, *J. Chem. Phys.* **96**, 4171 (1992).
- [20] A. Patkowski, W. Steffen, H. Nilgens, E. W. Fischer, and R. Pecora, *J. Chem. Phys.* **106**, 8401 (1997).
- [21] L. Comez, D. Fioretto, L. Verdini, P. A. Rolla, J. Gapinski, A. Patkowski, W. Steffen, and E. W. Fischer (unpublished).
- [22] R. Casalini, D. Fioretto, A. Livi, M. Lucchesi, and P. A. Rolla, *Phys. Rev. B* **56**, 3016 (1997).
- [23] F. Stickel, E. W. Fischer, and R. Richert, *J. Chem. Phys.* **102**, 6251 (1995); **104**, 2043 (1996).
- [24] C. Hansen, F. Stickel, T. Berger, R. Richert, and E. W. Fischer, *J. Chem. Phys.* **107**, 1086 (1997).
- [25] S. Capaccioli, S. Corezzi, G. Gallone, P. A. Rolla, L. Comez, and D. Fioretto, *J. Non-Cryst. Solids* (to be published).
- [26] F. Nizzoli and J. R. Sandercock, in *Dynamical Properties of Solids*, edited by G. Horton and A. A. Maradudin (North-Holland, Amsterdam, 1990).
- [27] See, for example, *Phenomena Induced by Intermolecular Interactions*, edited by G. Birnbaum (Plenum Press, New York, 1985).
- [28] B. J. Berne and R. Pecora, *Dynamic Light Scattering* (Wiley, New York, 1976).
- [29] L. Comez, D. Fioretto, L. Verdini, and P. Rolla, *J. Phys.: Condens. Matter* **9**, 3973 (1997).
- [30] L. Comez, D. Fioretto, L. Palmieri, G. Socino, and L. Verdini, in *1997 IEEE Ultrasonics Symposium Proceedings*, edited by S. C. Schneider, M. Levy, and B. R. McAvoy (IEEE, New York, in press), p. 731.
- [31] N. J. Tao, G. Li, and H. Z. Cummins, *Phys. Rev. B* **45**, 686 (1992).
- [32] C. J. Montrose, V. A. Solov'yev, and T. A. Litovitz, *J. Acoust. Soc. Am.* **43**, 117 (1968).
- [33] J. A. Forrest, K. Dalnoki-Veress, J. R. Stevens, and J. Dutcher, *Phys. Rev. Lett.* **77**, 2002 (1996).
- [34] The compliance and not the longitudinal modulus has been written in terms of HN relaxation functions for a direct comparison with dielectric measurements. It is well known, indeed, that both shape and frequency position of the functions relative to the same relaxation process assume different values if using the modulus or the compliance formalism. See, for instance, N.G. McCrum, B.E. Read, and G. Williams, *Unelastic and Dielectric Effects in Polymeric Solids* (Dover, New York, 1991), p. 109.
- [35] A. Schönhals, F. Kremer, A. Hofmann, E. W. Fischer, and E. Schlosser, *Phys. Rev. Lett.* **70**, 3459 (1993); A. Schönhals, F. Kremer, and E. Schlosser, *ibid.* **67**, 999 (1991); A. Schönhals and E. Schlosser, *Colloid Polym. Sci.* **267**, 125 (1989); **267**, 963 (1989).
- [36] S. Havriliak, Jr. and S. J. Havriliak, *J. Non-Cryst. Solids* **172-174**, 297 (1994).
- [37] A.K. Jonscher, *Universal Relaxation Law* (Chelsea Dielectric Press, London, 1996).

- [38] F. Alvarez, A. Alegría, and J. Colmenero, *Phys. Rev. B* **47**, 125 (1993); **44**, 7306 (1991).
- [39] E. Butta, A. Livi, G. Levita, and P. A. Rolla, *J. Polym. Sci., Part B: Polym. Phys.* **33**, 2253 (1995); J. M. Pochan, R. J. Gruber, and D. F. Pochan, *J. Polym. Sci., Polym. Phys. Ed.* **19**, 143 (1981).
- [40] N. J. Tao, G. Li, and H. Z. Cummins, *Phys. Rev. Lett.* **66**, 1334 (1991).
- [41] Y. Scheyer, C. Levelout, J. Pelous, J. C. Cook, M. Johnson, F. Prochazka, and D. Durand, *Physica B* **234**, 445 (1997).
- [42] X. Masood *et al.*, *Adv. Mol. Relax. Processes* **9**, 29 (1976).
- [43] R. Garwe, A. Schnhals, M. Beiner, K. Schrter, and E. Donth, *J. Phys.: Condens. Matter* **6**, 6941 (1994); F. Garwe, A. Schnhals, H. Lockwenz, M. Beiner, K. Schrter, and E. Donth, *Macromolecules* **29**, 247 (1996).
- [44] A. Arbe, D. Richter, J. Colmenero, and B. Farago, *Phys. Rev. E* **54**, 3853 (1996).
- [45] M. Schulz and E. Donth, *J. Non-Cryst. Solids* **168**, 186 (1994).
- [46] E. W. Fischer, E. Donth, and W. Steffen, *Phys. Rev. Lett.* **68**, 2344 (1992); E. J. Donth, *Relaxation and Thermodynamics in Polymers: Glass Transition* (Akademie-Verlag, Berlin, 1992).